Tailoring gas tungsten arc weld geometry using a genetic algorithm and a neural network trained with convective heat flow calculations

S. Mishra [1], T. DebRoy [*]

Department of Materials Science and Engineering, The Pennsylvania State University, University Park, PA 16802, United States

Abstract

Weld attributes like geometry and cooling rate are strong functions of the welding process parameters such as arc current, voltage and welding speed. A specific weld pool geometry can be produced using multiple sets of these welding variables, i.e., different combinations of arc current, voltage and welding speed. At present, there is no systematic methodology that can determine, in a realistic time frame, these multiple paths based on scientific principles. Here we show that multiple combinations of welding variables necessary to achieve a target gas tungsten arc (GTA) weld geometry can be systematically computed by a real number based genetic algorithm and a neural network that has been trained with the results of a heat transfer and fluid flow model. The neural network embodies the power of a numerical heat transfer and fluid flow model of GTA welding, since it can predict the fusion zone geometry, peak temperature and cooling rate and its input and output variables are consistent with the equations of conservation of mass, momentum and energy. A genetic algorithm is used to determine a population of solutions by minimizing an objective function that represents the difference between the calculated and the desired values of weld pool penetration and width. The use of a neural network in place of a heat transfer and fluid flow model significantly expedites the computational task. The desired weld geometry could be obtained with various combinations of welding variable sets. The computational methodology described here enables fabrication of a weld with desired geometry within the framework of phenomenological laws via alternative paths involving multiple combinations of welding variables.
© 2006 Elsevier B.V. All rights reserved.

Keywords: Weld geometry; Tailoring; Neural network; Genetic algorithm; Heat transfer; Fluid flow; GTAW

1. Introduction

In recent decades, systematic correlations between welding variables and weld characteristics have been attempted by numerical modeling of heat and fluid flow [1–19]. The numerical models have provided significant quantitative insights in the welding processes and the welded materials. These models have accurately predicted temperature and velocity fields, weld pool geometry, cooling rate, peak temperature, phase transformations [4,16], grain structure [6,7], and weld metal composition change owing to both the evaporation of alloying elements and the dissolution of gases [8]. Although, these powerful models have provided significant insight about the effect of various welding variables, their applications have been rather limited [20–22]

for several reasons. First, the models are comprehensive and require significant amount of computer time. Second, they are designed to calculate temperature and velocity fields for a given set of welding variables, i.e., they are unidirectional in nature. In other words, they cannot predict the welding variables needed to achieve a target weld geometry [20–22] or other weld attributes. Finally, the GTA welding system is highly complex and involves non-linear interaction of several welding variables. As a result, a particular weld attribute such as the geometry can be obtained via multiple paths, i.e., through the use of various sets of welding variables. What is needed, and not currently available, is for the models to have a capability to offer various choices of welding variable combinations, each capable of producing a target weld attribute.

Three main requirements need to be satisfied by a model for systematic tailoring of a weld attribute such as weld geometry based on scientific principles. First, the model should be capable of capturing all the major complex physical processes occurring during the GTA welding. Second, the model must have a bi-directional capability. In other words, in addition to

* Corresponding author. Tel.: +1 814 865 1974; fax: +1 814 865 2917.
  E-mail address: debroy@matse.psu.edu (T. DebRoy).
[1] Present address: Department of Metallurgical Engineering and Materials Science, Indian Institute of Technology Bombay, Mumbai, India.

the capability of the traditional unidirectional, forward models to compute the weld shape and size from a given set of welding variables, it should also have the inverse modeling ability, i.e., it should be able to systematically predict welding variables needed to produce a target weld geometry. Finally, the model must be able to determine various welding variable sets needed to attain a target weld geometry within a reasonable time.

Since multiple paths can lead to a target weld geometry [20–22], the classical gradient-based search and optimization methods that produce a single optimum solution cannot be used. These methods use a point-by-point approach, where one relatively imperfect solution in each iteration is modified to a different more appropriate solution [23,24]. Therefore, a combination of a classical optimization method with a phenomenological model can provide only a single local optimum solution in situations where multiple solutions exist. In contrast, genetic algorithms (GA) can obtain a population of optimal solutions [23–26]. In the context of welding, a GA can systematically search for multiple combinations of welding variable sets that comply with the phenomenological laws of welding physics and improve with iterations [20–22].

Recently, Kumar and DebRoy [20] and Mishra and DebRoy [21,22] developed bi-directional phenomenological models of gas metal arc (GMA) fillet welding and GTA butt welding, respectively, by coupling a genetic algorithm based optimization method with three-dimensional heat transfer and fluid flow models. They showed that the above approach can predict multiple combinations of welding variables to achieve a target geometry. However, these models [20–22] are unsuitable for practical applications, since they require several days of computer calculations. Kumar and DebRoy [20] used a parallel computing facility, i.e., running their model on multiple processors simultaneously to reduce computational time. Since it is very hard to maintain such a sophisticated computing facility in a manufacturing industry, their model can only be used for research purposes. Unless a model can do calculations in a reasonable time, it is unlikely to find widespread practical applications.

In GTA welding, the effect of welding variables on the weld geometry is non-linear and highly complex. A well-trained and rigorously tested neural network [27–30] can be used in place of a phenomenological model to capture the correlations between different welding variables and weld attributes. The neural network models are able to predict the outputs for different welding conditions rapidly [27–30]. With the improvements in computational hardware in recent years, a large volume of training and validation data can be generated with a well-tested numerical heat transfer and fluid flow model in a realistic time frame. A neural network trained with the results of a numerical heat transfer and fluid flow model can correlate various output variables such as the weld pool geometry, cooling rate, liquid velocities and peak temperatures with all the major welding variables and material properties. Furthermore, such correlations satisfy the basic scientific phenomenological laws expressed in the equations of conservation of mass, momentum and energy.

We show here that multiple sets of welding variables that are capable of producing a target weld geometry can be calculated in a realistic time frame by coupling a genetic algorithm with a neural network model of GTA welding that has been trained with the results of a well tested heat transfer and fluid flow model.

2. Mathematical model

The main computational engine used here is a neural network model [27], which is trained and validated using the results of a well-tested heat transfer and fluid flow model [8,12,17]. The details of the neural network model have been described elsewhere and are not repeated here. Only the salient features of the model necessary for tailoring the geometry of the fusion zone are briefly discussed here. The neural network model includes all the welding variables and material properties as input and provides weld dimensions, peak temperatures, maximum velocities and the cooling rates between 800 and 500 °C. This network has 17 input parameters, which are connected to output layer through a hidden layer of 14 nodes as shown in Fig. 1. A hyperbolic tangent function (which is a symmetric sigmoid function) is used as the activation function to include the non-linear behavior of different variables. A back-propagation algorithm [27,31–34] was used to update the synaptic weights of the neural network. The algorithm used a hybrid method involving a genetic algorithm and a gradient descent technique to reduce the mean square error, MSE, between the actual outputs (d) and predicted values (o) [27]:

$$\text{MSE} = \frac{1}{q}\sum_q (d_{qk} - o_{qk})^2 \tag{1}$$

where q represents the number of training datasets and k represents the number of output nodes, which is one in this work. The hybrid algorithm reduces the training time as the gradient descent method takes advantage of gradient information to calculate the optimal solution, whereas the genetic algorithm helps to avoid local minima [27]. The resulting neural network is computationally more efficient than a phenomenological heat
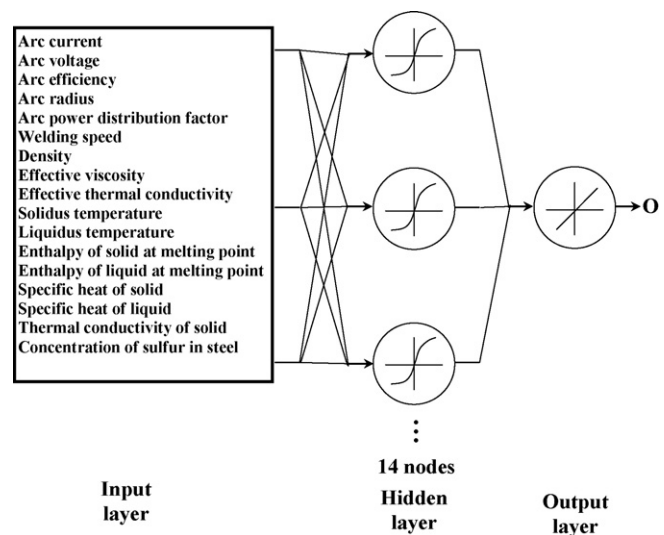
Fig. 1. The architecture of the neural network model used in this work. The input layer has 17 input variables, which is connected to a hidden layer. The output of the network is either weld pool penetration or width.

Table 1
Terminology used in genetic algorithm

Biological terms	Equivalent welding variables and representation in genetic algorithm
Genes: units containing hereditary information	In the form of non-dimensional variables, f_1, f_2 and f_3. E.g., $f_1 = 1.10$; $f_2 = 1.70$; $f_3 = 1.56$
Chromosome/individual: a number of genes folded together	A set of input variable values taken together, i.e., (1.10, 1.70, 1.56)
Population: collection of many chromosomes/individuals	Collection of multiple sets: (1.10, 1.70, 1.56), (1.20, 1.54, 1.65), ... (1.23, 1.65, 1.75)
Parents: chromosomes/individuals participating for creating new individuals (or offsprings)	Parents: e.g., (1.10, 1.70, 1.56), (1.23, 1.65, 1.75)
Objective function value: value of objective function determines if a chromosome/individual survives or dies	Objective function: calculated for each set of input variables using Eq. (2)

transfer and fluid flow model as it significantly expedites the computational speed. For example, for a given set of welding parameters, the phenomenological heat transfer and fluid flow model takes more than 5 min to calculate the weld pool geometry, while the same calculation can be done by the neural network in less than 1 s. Furthermore, the results from the neural network model match with the corresponding results from the heat and fluid flow model.

The genetic algorithm (GA) based search for multiple sets of welding variables to achieve a target weld geometry starts with many initial sets of randomly chosen values of the three most important welding variables, i.e., arc current, voltage and welding speed. A systematic global search is next undertaken to find multiple sets of values of these three welding variables that lead to least error between the calculated and the target weld dimensions, i.e., penetration and width. The neural network model cal-

culates the values of these weld dimensions for each set of input welding variables. The chosen values of welding variables do not always produce the desired weld dimensions and the resulting mismatch between the computed and the desired weld dimensions is expressed by the following objective function, $O(f)$:

$$O(f) = \left(\frac{p^c}{p^t} - 1 \right)^2 + \left(\frac{w^c}{w^t} - 1 \right)^2 \tag{2}$$

where p^c and w^c are the computed penetration and width of the weld bead, respectively, and p^t and w^t are the corresponding target or desired values of these attributes. The objective function, $O(f)$, depends on the three main welding variables, i.e., arc current, I, voltage, V, and welding speed, U:

$$O(f) = O(f_1, f_2, f_3) = O \left(\frac{I}{I_r}, \frac{V}{V_r}, \frac{U}{U_r} \right) \tag{3}$$
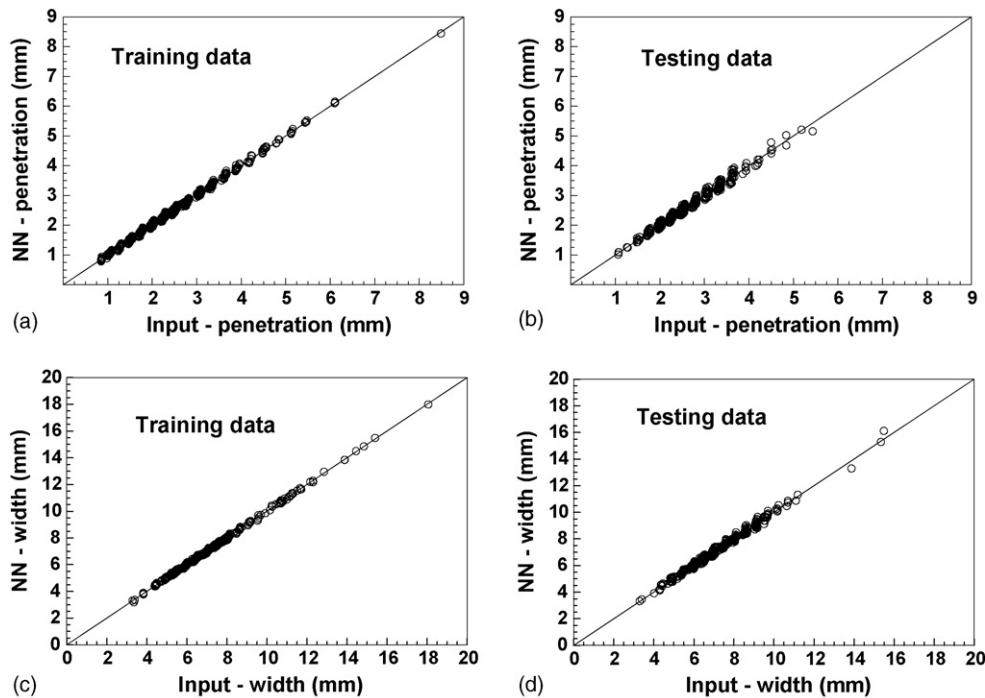
Fig. 2. Comparison of output variables, i.e.: (a) penetration–training dataset, (b) penetration–testing dataset, (c) width–training dataset, and (d) width–testing dataset, calculated by heat transfer and fluid flow model (x-axis) with corresponding values predicted by neural network (NN) model of GTA butt welding. The diagonal lines in each plot show that ideally all the points should lie on this line. The training data and the testing data comprise of 1250 and 500 datasets, respectively.

In Eq. (3), the reference values, I_r, V_r and U_r represent the order of magnitude of the welding variables. Note that Eq. (3) is made non-dimensional to preserve the importance of all three welding variables by making their non-dimensional values comparable in magnitude. The GA produces new individuals, or sets of welding conditions, with iterations based on the evolutionary principles [20–22,24–26]. The GA used in the present study is a parent centric recombination (PCX) operator based generalized generation gap (G3) model [20–22,24–26]. This model was chosen because it has been shown to have a faster convergence rate on standard test functions as compared to other evolutionary algorithms and classical optimization algorithms [24,25]. The specific application of this model for obtaining the multiple sets of welding variables to achieve a target weld geometry is described in Appendix A. Table 1 provides explanations of various terms used in GA as related to welding.

3. Results and discussion

The neural network used here was trained and validated with results from a well-tested three-dimensional numerical heat transfer and fluid flow model. Separate feed forward neural networks were developed [27], one each for predicting penetration and width of GTA butt welds to achieve high accuracies in the calculation of these output parameters. The weights in the neural network models were calculated using a hybrid optimization scheme involving the gradient descent (GD) method and a

genetic algorithm (GA) [27]. The hybrid optimization scheme helped in finding optimal weights through a global search as evidenced by good agreement between all the outputs from the neural networks and the corresponding results from the heat and fluid flow model [27] as shown in Fig. 2. The neural network model provided correct values of penetration and width for various combinations of welding variables I, V and U.

It has been shown in the literature [20–22] that by coupling a genetic algorithm (GA) based optimization method with three-dimensional heat transfer and fluid flow models, multiple combinations of welding variables could be predicted to achieve a target weld geometry with good accuracy, with objective function values less than 0.01. This is possible because GA can provide a population of solutions. In the present study, the neural network model was combined with a real number based
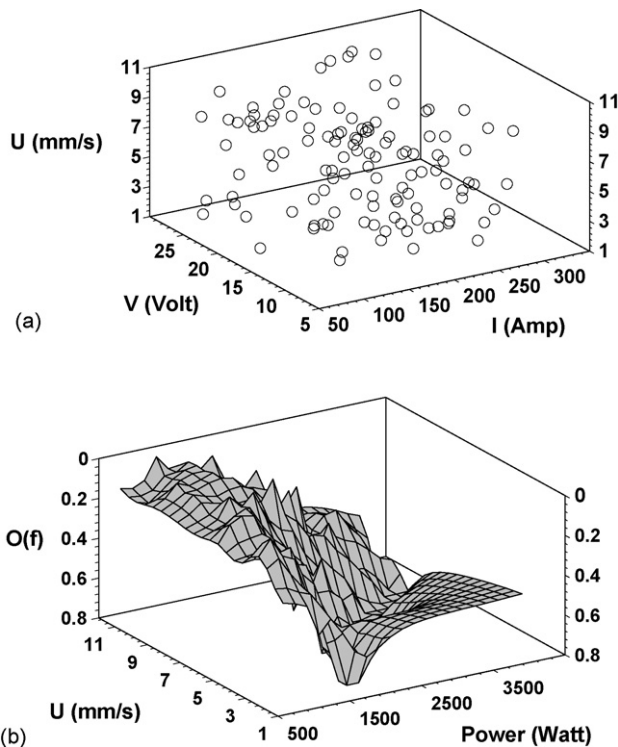
Fig. 3. Initial values of individual welding variable sets and their objective functions. (a) A large space of variables was searched to find optimum solutions as shown by 120 randomly selected initial welding variable sets. (b) The low values of the objective functions of several individuals in the initial population indicate the possibility of existence of multiple optimal solutions.
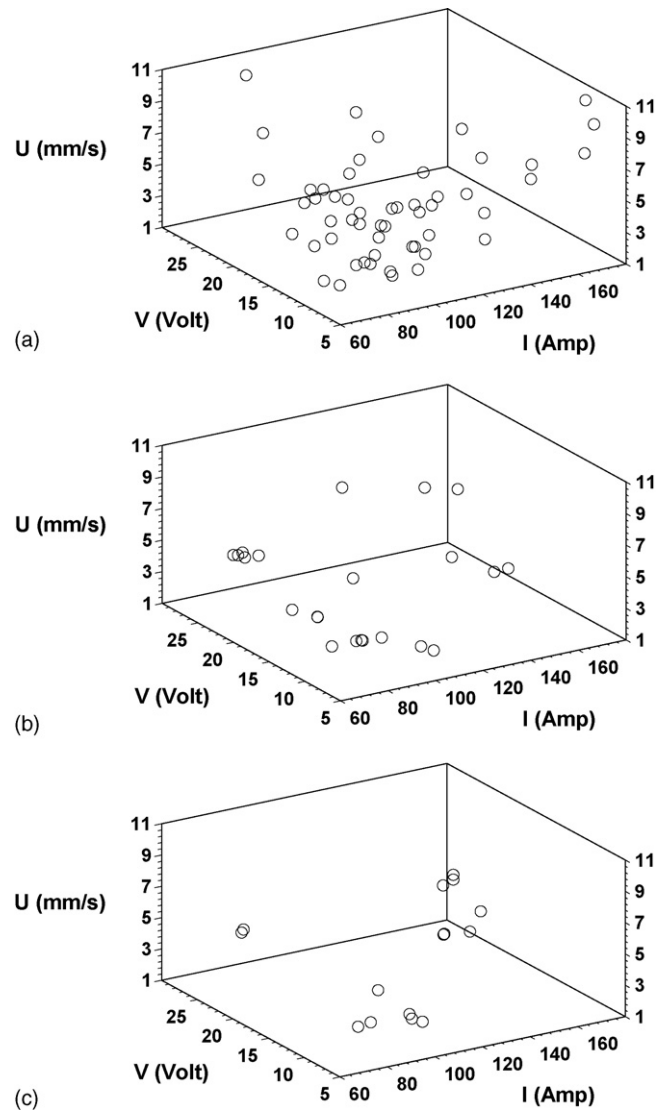
Fig. 4. Several fairly diverse welding variable sets could produce low values of the objective function indicating the existence of alternate paths to obtain the target weld geometry. The plots show the welding variable sets that produced low values of the objective function, $O(f)$, with iterations: (a) individuals after 1st iteration with $O(f)$ less than 0.1, (b) individuals after 10th iteration with $O(f)$ less than 0.01, and (c) individuals after 25th iteration with $O(f)$ less than 0.001.

Table 2
Various combinations of welding variables, i.e., arc current (I), voltage (V) and welding speed (U) obtained using neural network model to achieve the following target weld dimensions: penetration = 1.39 mm and width = 4.05 mm

Individual solutions	I (A)	V (V)	U (mm/s)	Penetration (mm)	Width (mm)
(a)	102.6	9.8	3.4	1.40	4.08
(b)	86.6	23.3	9.0	1.39	4.06
(c)	97.2	10.1	3.2	1.39	4.04
(d)	133.6	11.4	9.6	1.39	4.06
(e)	115.6	10.2	5.1	1.39	4.05
(f)	126.8	10.3	6.7	1.39	4.05
(g)	88.6	9.7	2.2	1.39	4.04
(h)	94.3	9.5	2.6	1.39	4.06

The target weld geometry was obtained experimentally using the following welding variables: I = 101.0 A, V = 9.9 V and U = 3.4 mm/s for GTA welding of 303 stainless steel (0.3 wt.% sulfur).

GA to tailor weld geometry. The effectiveness of the approach was tested by finding different sets of welding variables, which could provide a specified weld geometry. The computational task involved three steps. First, a target weld geometry was selected by specifying one set of values of penetration and width. Second, the model was run to obtain multiple combinations of welding variable sets each of which could produce the target weld geometry. Third, and final, the results obtained from the model were adequately verified. These three steps are explained in detail in the following discussion.

To start the calculation, the specification of a target geometry was necessary. It involved stating realistic combinations of the weld penetration and width. To test the model, these weld dimensions from an actual welding experiment were specified as a target geometry. The target weld geometry was obtained experimentally using the following welding variables: I = 101.0 A, V = 9.9 V and U = 3.4 mm/s for GTA welding of 303 stainless steel (0.3 wt.% sulfur), and the resulting weld dimensions were: penetration = 1.39 mm and width = 4.05 mm. If the model works correctly, the various combinations of welding variables obtained from the model must include a set of welding variables that are fairly close to the set of variables used in the experiment. It should be noted that the ability of the model to produce this solution is only a necessary, but not sufficient component of the model verification. Since the model produces multiple solutions, other solutions obtained from the model have to be verified by comparing the calculated weld geometry with the experimentally obtained geometry.

In the next step (i.e., second step), a population of 120 individuals was defined to start the operation of GA. This number of variable sets was determined based on how the population size influences the effectiveness of GA using standard test functions [24,25]. Each individual in the population contained a set of randomly chosen welding variables, i.e., arc current, voltage and welding speed. Fig. 3(a) shows the initial values of the individuals, i.e., sets of I, V and U. Values of the welding variables I, V and U were chosen randomly in the range of 75–300 A, 8–30 V and 1.7–10.0 mm/s, respectively. Such large ranges of values were chosen for the welding variables in order to explore a large domain of welding variables to include all possible solutions and also to maintain diversity in the solutions. These welding variable sets were then improved iteratively using a combination of GA and the neural network. The progress of the iterations was monitored by calculating the objective function values, defined in Eq. (2), for each set of welding variables. An individual with a low objective function value indicates that the I, V and U values it contains result in a small discrepancy between the computed and the target weld geometry. Fig. 3(b) shows that for many sets of welding variables, the computed values of the objective function, $O(f)$, are fairly low, indicating that each of these variable sets can produce a weld geometry that is close to the target geometry.

Fig. 4(a)–(c) indicates several welding variable sets that have progressively lower objective function values. The objective function values are lower than 0.1, 0.01 and 0.001, corresponding to the 1st, 10th and 25th generation of individuals, respectively. It is noteworthy that in Fig. 4, the sets of welding

Table 3
Various combinations of welding variables, i.e., arc current (I), voltage (V) and welding speed (U) obtained using neural network model to achieve the following target weld dimensions: penetration = 1.94 mm and width = 4.39 mm

Individual solutions	I (A)	V (V)	U (mm/s)	Penetration (mm)	Width (mm)
(a)	124.3	9.4	3.0	1.94	4.39
(b)	79.3	16.0	3.1	1.94	4.37
(c)	99.9	9.8	1.7	1.94	4.33
(d)	116.4	9.3	2.5	1.94	4.38
(e)	145.7	9.0	4.2	1.94	4.36
(f)	89.3	12.4	2.3	1.94	4.36
(g)	107.0	9.6	2.1	1.94	4.37
(h)	175.9	8.6	6.0	1.94	4.37

The target weld geometry was obtained using the welding conditions listed in (a).

variables are distributed throughout the welding variable space, signifying the existence of multiple paths to attain the specified weld geometry. The progressive reduction of the objective function values of the best individuals indicates that the solutions are improved with iterations. The calculation was continued until 5% individuals in the population had the value of objective function less than 1.0×10^{-5}. The chosen value of the objective function ensured sufficient accuracy within the practical limits of experimental errors. The calculated combinations of the welding variables, which constitute the final solutions, are presented in Table 2. The calculations required less than 1 min in a PC with 3.0 GHz Intel P4 CPU and 1024 MB PC2700 DDR-SDRAM memory. It is useful to recall that several days of computational time was required on the same machine by a model developed
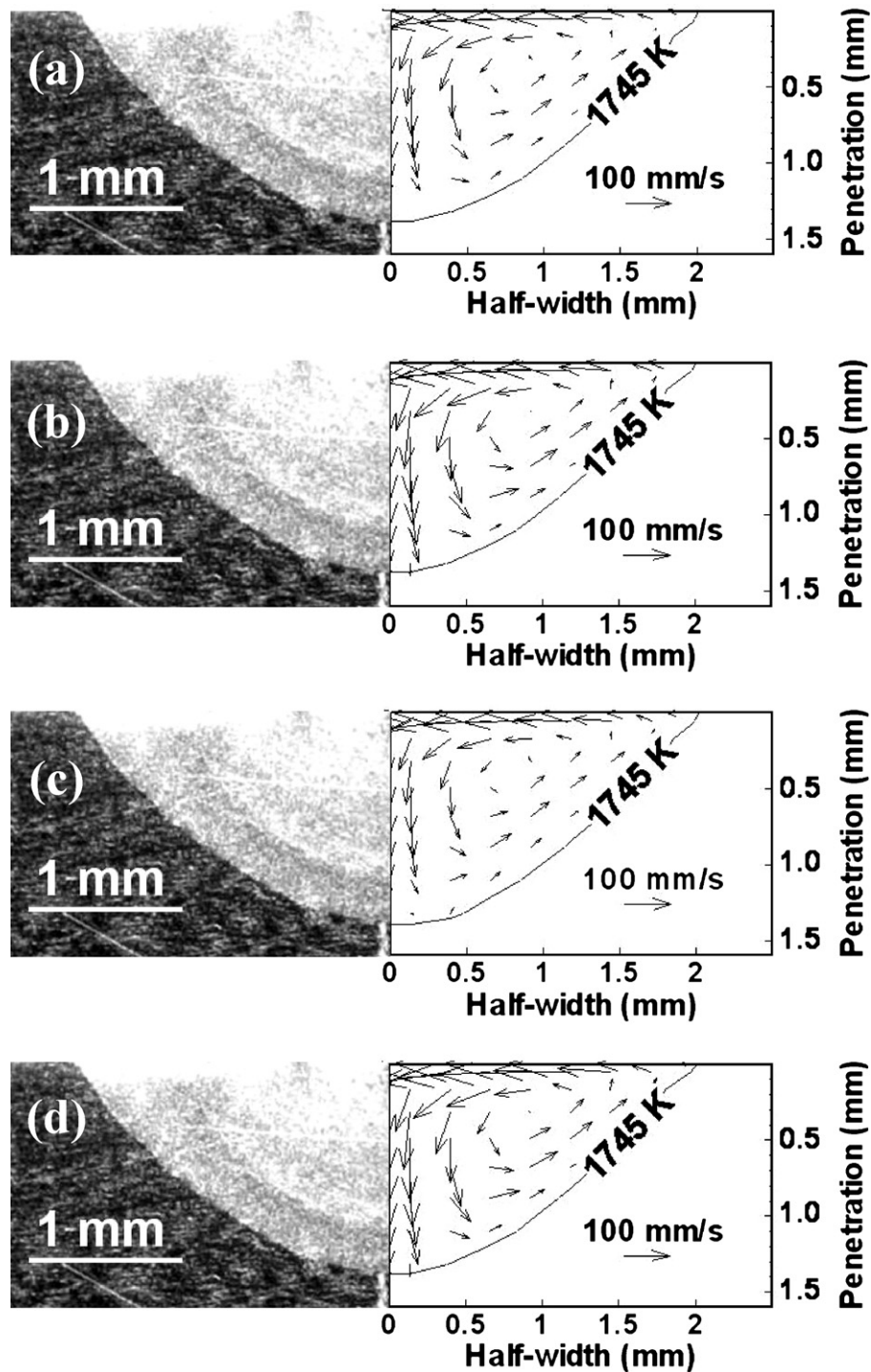
Fig. 5. Comparison of the experimental target weld geometry with those calculated from a well-tested heat transfer and fluid flow model for GTA welding [8,12,17]. Calculated weld geometries in cases (a)–(h) correspond to the eight solutions, i.e., sets of current, voltage and welding speed listed in Table 2. In the calculated results the weld pool boundary is marked by the 1745 K isotherm, which is the solidus temperature of stainless steel.
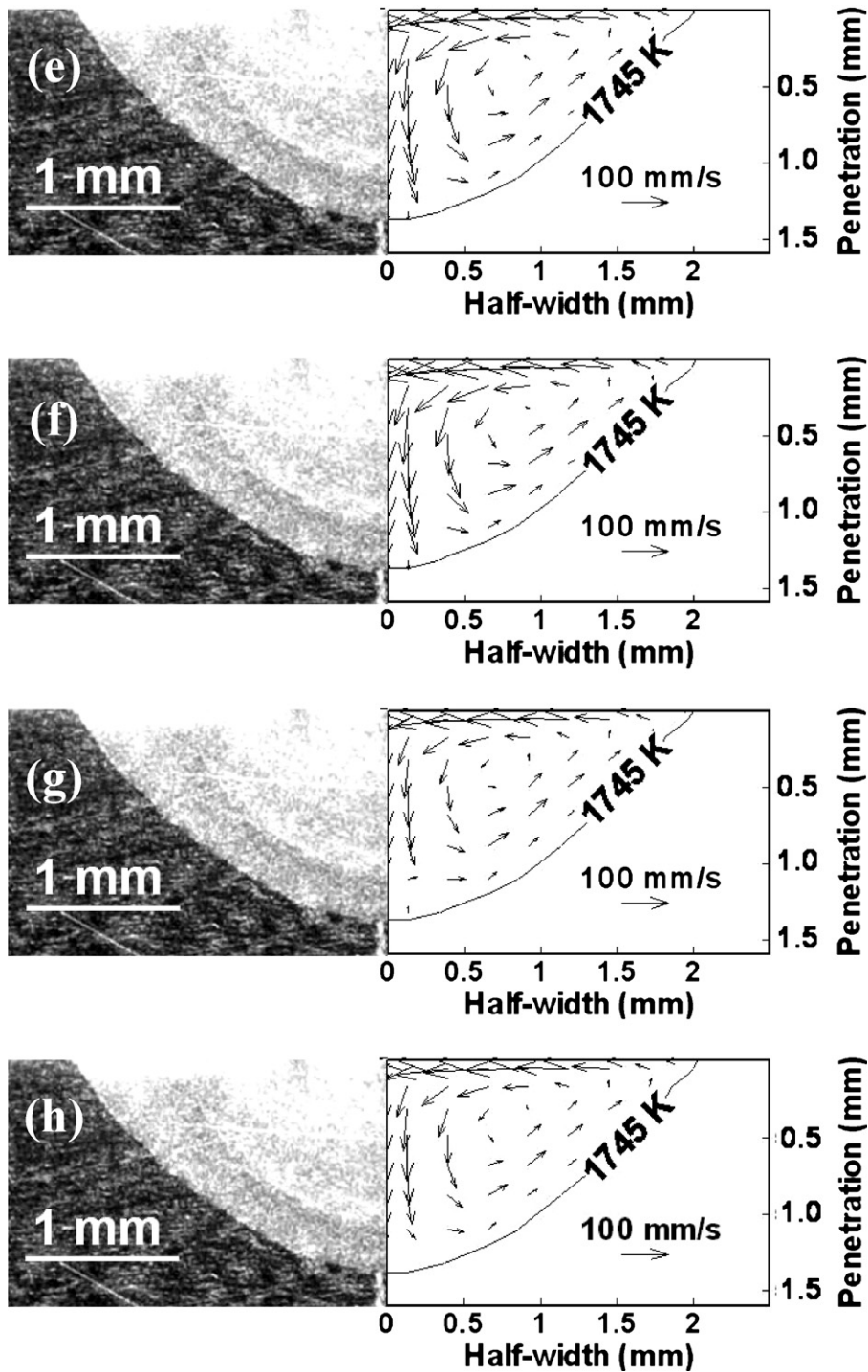
Fig. 5. (*Continued*).

by Mishra and DebRoy [27] that used a numerical heat transfer and fluid flow model. This time saved by using a neural network justifies its use as a forward model in place of a heat transfer and fluid flow model.

The third step involved verification of the computed solutions. Since the target geometry was produced by conducting an experiment, an initial test is to check if the population of solutions produced by the model includes a set of welding variables that is very close to, if not the same as, that used to produce

the weld. Note that the values of arc current, voltage and welding speed in solution (a) of Table 2 are almost the same as the corresponding experimental values. Each solution, i.e., a set of current, voltage and welding speed, listed in Table 2, was used to calculate the geometric parameters, i.e., penetration and width of the weld using the neural network. The computed geometric parameters were compared with those produced in the experiment. Table 2 shows that for each set of computed welding conditions, the corresponding geometric parameters agreed well

with the desired experimental values. In order to further test the accuracy of the solutions, i.e., sets of current, voltage and welding speed listed in Table 2, the weld geometry for each case was calculated from a well-tested heat transfer and fluid flow model for GTA welding [8,12,17]. These calculated weld geometries were compared with the experimental target weld geometry, as shown in Fig. 5(a)–(h). The calculated weld pool boundary is marked by the solidus temperature of stainless steel, i.e., 1745 K. Fig. 5 shows that all the optimized solutions listed in Table 2 result in the correct prediction of the target weld shape and size. Furthermore, the solutions in Table 2 exhibit significantly different values of the welding variables indicating the diversity of the paths through which the specified geometry can be obtained. For example, Table 2 shows that the current values ranged from 86.6 to 133.6 A, voltages varied between 9.5 and 23.3 V and welding speed changed from 2.2 to 9.6 mm/s in various sets of optimized values. The fact that all these diverse viable paths can lead to the same weld pool dimensions clearly indicates the complexity and significant non-linearity of the fusion welding system.

A similar exercise was also undertaken where a hypothetical weld geometry represented by a penetration of 1.94 mm and a width of 4.39 mm was produced by a current of 124.3 A, voltage of 9.4 V and welding speed of 3.0 mm/s in 304RL stainless steel (0.11 wt.% sulfur). Table 3 lists all other combinations of welding variables, i.e., solutions (b)–(h) that can produce this geometry. The values of the welding variables differed considerably from each other. For example, current, voltage and welding speed varied among solutions by 38%, 30% and 55%, respectively. All these differences in the important welding variables indicate significant diversity in the paths, all of which lead to the same set of target weld dimensions.

4. Conclusions

A bi-directional model of gas tungsten arc (GTA) welding was developed by coupling a neural network model with a real number based genetic algorithm to calculate the welding conditions needed to obtain a target weld geometry. Unlike conventional neural network models that are trained with experimental data, which predict weld geometry for a particular set of welding conditions, the proposed model could estimate the welding conditions necessary for obtaining a target weld geometry within the framework of phenomenological laws.

The model was used to determine multiple sets of welding variables, i.e., combinations of arc current, voltage and welding speed to obtain a specified weld geometry. It was found that a specific weld geometry was attainable via multiple pathways involving various sets of welding variables. Furthermore, these sets of welding variables involved significantly different values of current, voltage and welding speed. The use of a neural network model in place of heat transfer and fluid flow model reduced the computation time and provided the solution within 1 min. This makes the model practically usable for welding engineers in the industry. Good agreement between the model predictions and the experimental data of weld pool penetration and width for various welding conditions shows that this approach is promising. Although the work reported here focuses on tailoring of weld geometry, these results provide hope that the science based tailoring of structure and properties of weldments may also become attainable in the future.

Appendix A. PCX based G3 genetic algorithm

The GA used in the present study to calculate the optimized values of the input welding variables is a parent centric recombination (PCX) operator based generalized generation gap (G3) model [24,25]. The algorithm for the model is as follows:

(1) A population is a collection of many individuals and each individual represents a set of randomly chosen values of the three input variables, i.e., arc current, voltage and welding speed. A parent refers to an individual in the current population. The best parent is the individual that has the best fitness, i.e., gives the minimum value of the objective function, defined by Eq. (2), in the entire population. The best parent and two other randomly selected parents are chosen from the population.
(2) From the three chosen parents, two offsprings or new individuals are generated using a recombination scheme. PCX based G3 models are known to converge rapidly when three parents and two offsprings are selected [24,25]. A recombination scheme is a process for creating new individuals from the parents.
(3) Two new parents are randomly chosen from the current population.
(4) A subpopulation of four individuals that includes the two randomly chosen parents in step (3) and two new offsprings generated in step (2) is formed.
(5) The two best solutions, i.e., the solutions having the least values of the objective function, are chosen from the subpopulation of four members created in step (4). These two individuals replace the two parents randomly chosen in step (3).
(6) The calculations are repeated from step (1) again until convergence is achieved.

The above steps, as applied to the present study, are shown in Fig. 6. The working of the model to find the multiple sets of welding variables by minimizing the objective function is illustrated in Fig. 7. The recombination scheme (step (2)) used in the present model is based on the parent centric recombination (PCX) operator [24,25]. A brief description of the PCX operator, as applied to the present problem, is given as follows.

First, three parents, i.e., (f_1^0, f_2^0, f_3^0), (f_1^1, f_2^1, f_3^1), (f_1^2, f_2^2, f_3^2) are randomly selected from the current population. Here, the subscripts represent the three input
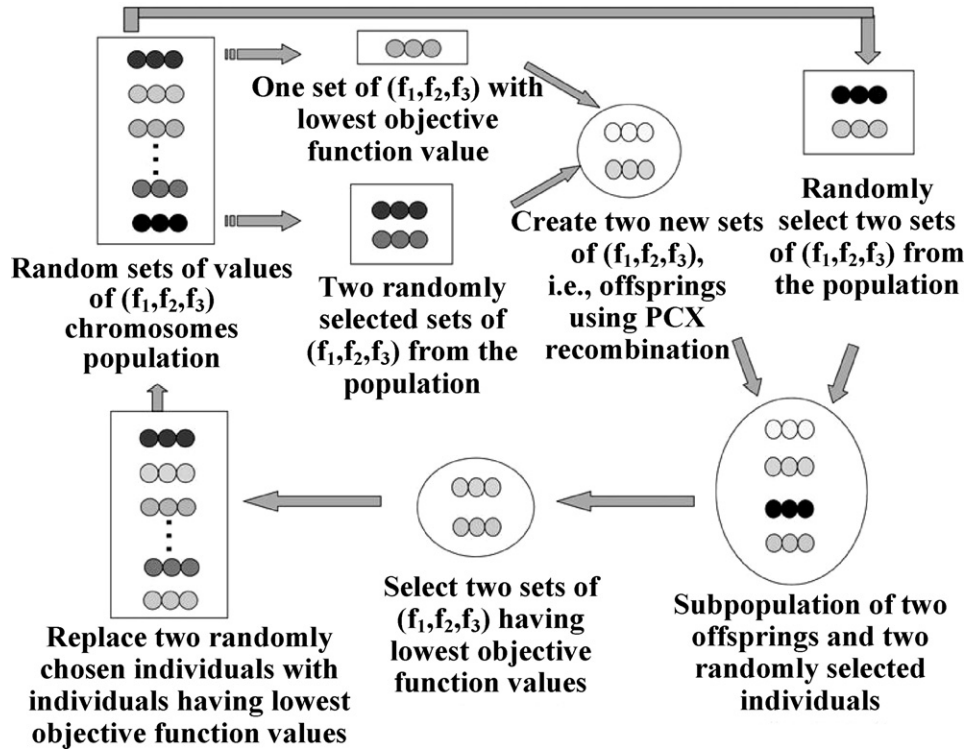
Fig. 6. The working principle of the genetic algorithm based on generalized generation gap (G3) model and using parent centric recombination (PCX) operator.
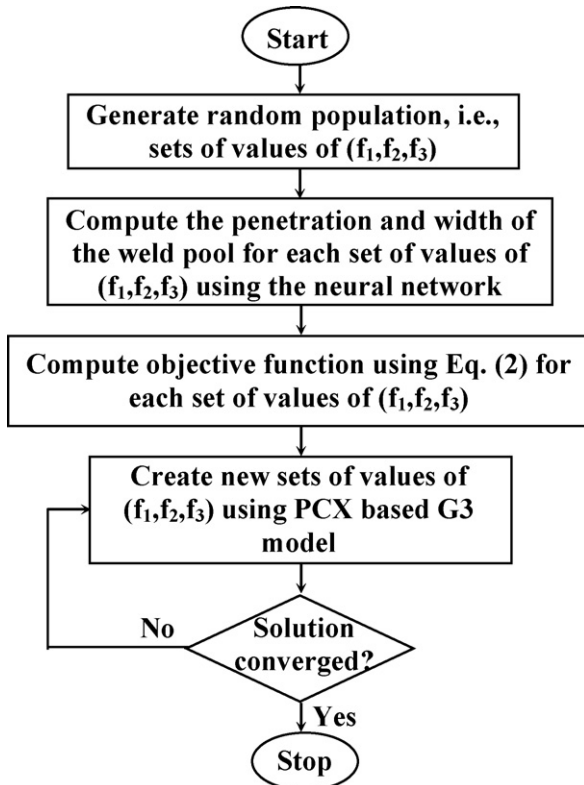
Fig. 7. Flowchart of the proposed model after coupling of generalized generation gap (G3) genetic algorithm with neural network model.

welding variables, while the superscripts denote the parent identification number. The mean vector or centroid, $\bar{g} = ((f_1^0 + f_1^1 + f_1^2)/3, (f_2^0 + f_2^1 + f_2^2)/3, (f_3^0 + f_3^1 + f_3^2)/3)$, of the three chosen parents is computed. To create an offspring, one of the parents, say $\vec{x}^{(p)} = (f_1^0, f_2^0, f_3^0)$ is chosen randomly. The direction vector, $\vec{d}^{(p)} = \vec{x}^{(p)} - \bar{g}$, is next calculated from the selected parent to the mean vector or centroid. Thereafter, from each of the other two parents, i.e., (f_1^1, f_2^1, f_3^1) and (f_1^2, f_2^2, f_3^2), perpendicular distances, D_i, to the direction vector, $\vec{d}^{(p)}$, are computed and their average, $\bar{D}$, is found. Finally, the offspring, i.e., $\bar{y} = (f_1', f_2', f_3')$, is created as follows:

$$\bar{y} = \vec{x}^{(p)} + w_\zeta \left| \vec{d}^{(p)} \right| + \sum_{i=1, i\neq p}^{3} w_\eta \bar{D} \vec{h}^{(i)} \tag{A1}$$

where $\vec{h}^{(i)}$ are the orthonormal bases that span the subspace perpendicular to $\vec{d}^{(p)}$, and w_ζ and w_η are randomly calculated zero-mean normally distributed variables. The values of the variables that characterize the offspring, $\bar{y} = (f_1', f_2', f_3')$, are calculated as follows:

$$f_1' = f_1^0 + f_{11} + f_{12} \tag{A2.a}$$

$$f_2' = f_2^0 + f_{21} + f_{22} \tag{A2.b}$$

$$f_3' = f_3^0 + f_{31} + f_{32} \tag{A2.c}$$

where

$$f_{11} = w_\zeta \left(\frac{2f_1^0 - f_1^1 - f_1^2}{3} \right) \tag{A3.a}$$

$$f_{21} = w_\zeta \left(\frac{2f_2^0 - f_2^1 - f_2^2}{3} \right) \qquad \text{(A3.b)}$$

$$f_{31} = w_\zeta \left(\frac{2f_3^0 - f_3^1 - f_3^2}{3} \right) \qquad \text{(A3.c)}$$

$$f_{12} = w_\eta \left(\frac{a_2 + b_2}{2} \right) \left[1 - \left(\frac{2f_1^0 - f_1^1 - f_1^2}{3d} \right)^2 \right] \qquad \text{(A3.d)}$$

$$f_{22} = w_\eta \left(\frac{a_2 + b_2}{2} \right) \left[1 - \left(\frac{2f_2^0 - f_2^1 - f_2^2}{3d} \right)^2 \right] \qquad \text{(A3.e)}$$

$$f_{32} = w_\eta \left(\frac{a_2 + b_2}{2} \right) \left[1 - \left(\frac{2f_3^0 - f_3^1 - f_3^2}{3d} \right)^2 \right] \qquad \text{(A3.f)}$$

The expressions for the variables d, a_2, and b_2, used in Eqs. (A3.d)–(A3.f), are as follows:

$$d = \sqrt{\left(\frac{2f_1^0 - f_1^1 - f_1^2}{3} \right)^2 + \left(\frac{2f_2^0 - f_2^1 - f_2^2}{3} \right)^2 + \left(\frac{2f_3^0 - f_3^1 - f_3^2}{3} \right)^2} \qquad \text{(A4.a)}$$

$$a_2 = e_1 \times \sqrt{1 - (a_1)^2} \qquad \text{(A4.b)}$$

$$b_2 = e_2 \times \sqrt{1 - (b_1)^2} \qquad \text{(A4.c)}$$

$$a_1 = \sum_{i=1}^{3} \frac{(f_i^1 - f_i^0)((2f_i^0 - f_i^1 - f_i^2)/3)}{d \times e_1} \qquad \text{(A4.d)}$$

$$e_1 = \sqrt{(f_1^1 - f_1^0)^2 + (f_2^1 - f_2^0)^2 + (f_3^1 - f_3^0)^2} \qquad \text{(A4.e)}$$

$$b_1 = \sum_{i=1}^{3} \frac{(f_i^2 - f_i^0)((2f_i^0 - f_i^1 - f_i^2)/3)}{d \times e_2} \qquad \text{(A4.f)}$$

$$e_2 = \sqrt{(f_1^2 - f_1^0)^2 + (f_2^2 - f_2^0)^2 + (f_3^2 - f_3^0)^2} \qquad \text{(A4.g)}$$

References

[1] A. De, T. DebRoy, Weld. J. 84 (2005) 101s–112s.
[2] W. Zhang, C.-H. Kim, T. DebRoy, J. Appl. Phys. 95 (2004) 5210–5219.
[3] W. Zhang, C.-H. Kim, T. DebRoy, J. Appl. Phys. 95 (2004) 5220–5229.
[4] W. Zhang, T. DebRoy, J.W. Elmer, Sci. Technol. Weld. Join. 10 (2005) 574–582.
[5] A. De, T. DebRoy, J. Phys. D 37 (2004) 140–150.
[6] S. Mishra, T. DebRoy, J. Phys. D 37 (2004) 2191–2196.
[7] S. Mishra, T. DebRoy, Acta Mater. 52 (2004) 1183–1192.
[8] X. He, P. Fuerschbach, T. DebRoy, J. Appl. Phys. 94 (2003) 6949–6958.
[9] S. Mishra, S. Chakraborty, T. DebRoy, J. Appl. Phys. 97 (2005) 94912–94920.
[10] A. Kumar, T. DebRoy, J. Appl. Phys. 94 (2003) 1267–1277.
[11] A. De, T. DebRoy, J. Appl. Phys. 95 (2004) 5230–5239.
[12] W. Zhang, G.G. Roy, J.W. Elmer, T. DebRoy, J. Appl. Phys. 93 (2003) 3022–3033.
[13] A. Kumar, W. Zhang, T. DebRoy, J. Phys. D 38 (2005) 118–126.
[14] A. Kumar, T. DebRoy, J. Phys. D 38 (2005) 127–134.
[15] X. He, J.W. Elmer, T. DebRoy, J. Appl. Phys. 97 (2005) 84909–84917.
[16] W. Zhang, T. DebRoy, T.A. Palmer, J.W. Elmer, Acta Mater. 53 (2005) 4441–4453.
[17] K. Mundra, T. DebRoy, K. Kelkar, Numer. Heat Transfer 29 (1996) 115–129.
[18] A. Kumar, T. DebRoy, Int. J. Heat Mass Transfer 47 (2004) 5793–5806.
[19] J.F. Lancaster, The Physics of Welding, 2nd ed., Pergamon, Oxford, 1986.
[20] A. Kumar, T. DebRoy, Metall. Mater. Trans. A 36 (2005) 2725–2735.
[21] S. Mishra, T. DebRoy, J. Phys. D 38 (2005) 2977–2985.
[22] S. Mishra, T. DebRoy, J. Appl. Phys. 98 (2005) 044902.
[23] D.E. Goldberg, Genetic Algorithm in Search, Optimization and Machine Learning, Addison-Wesley, MA, 1989.
[24] K. Deb, Multi-objective Optimization using Evolutionary Algorithms, Wiley, New York, 2001.
[25] K. Deb, A. Anand, D. Joshi, Evol. Comp. 10 (2002) 371–395.
[26] A. Kumar, S. Mishra, J.W. Elmer, T. DebRoy, Metall. Mater. Trans. A 36 (2005) 15–22.
[27] S. Mishra, T. DebRoy, Weld. J. 85 (2006) 231s–242s.
[28] A. Kumar, T. DebRoy, Weld. J. 85 (2006) 292s–304s.
[29] J.M. Vitek, Y.S. Iskander, E.M. Oblow, Weld. J. 79 (2000) 33–40.
[30] H.K.D.H. Bhadeshia, ISIJ Int. 39 (1999) 966–979.
[31] S. Haykin, Neural Network: A Comprehensive Foundation, Prentice Hall Publ., NJ, 1999.
[32] T. Masters, Practical Neural Network Recipes in C++, Academic Press, Boston, 1993.
[33] M.T. Hagan, Neural Network Design, PWS Publ., Boston, 1996.
[34] D.E. Rumelhart, G.E. Hinton, R.J. Williams, Nature 323 (1986) 533–536.